Peer review status:

This is a non-peer-reviewed preprint submitted to EarthArXiv.

Impact of Marine Heatwaves and Coldwaves on CO_2 in the South China Sea

Zhao Meng[a]

[a]Tsinghua Shenzhen International Graduate School, Tsinghua University, Shenzhen 518052, China

Abstract:

Global warming is increasing the frequency and intensity of marine heatwaves (MHWs) in the South China Sea, while marine cold waves (MCWs) occur intermittently. Both phenomena influence the air-sea CO_2 flux (FCO2) at the air-sea interface. This study uses inversion and reanalysis data, along with FCO2 diagnostic methods, to assess their impact on FCO2 in the South China Sea from 2003 to 2019. The results show that MHWs enhance CO_2 release (+0.016 mmol/m²/d), whereas MCWs reduce it (-0.14 mmol/m²/d). The variation in FCO2 is primarily controlled by the sea-air partial pressure difference (ΔpCO2) during both MHWs and MCWs, with the surface seawater CO_2 partial pressure (pCO2sea) being the main factor influencing ΔpCO2. Specifically, MHWs increase pCO2sea, thus increasing ΔpCO2, while MCWs decrease pCO2sea, lowering ΔpCO2. Additionally, temperature factors were the primary drivers of changes in pCO2sea during both MHWs and MCWs, with their impact gradually intensifying over time. The South China Sea serves not only as a representative of a low-latitude marginal sea but also as a "mini-ocean," making these findings valuable for broader oceanographic research.

Key Words:

Marine heatwaves, marine coldwaves, air-sea CO_2 fluxes, South China Sea

1、Introduction

Against the backdrop of global warming, the duration and frequency of global marine heatwaves (MHWs) are increasing, leading to intensified impacts and garnering widespread attention (Frölicher et al., 2018; Oliver et al., 2018; Hu et al.,

2021; Amaya et al., 2023; Oliver et al., 2021; Zhao et al., 2023). The concept of MHW was introduced by Pearce et al., (2011) to describe an abnormal warming event in seawater. Such events are typically defined as periods in which sea surface or upper ocean temperatures persist above fixed thresholds, seasonal change thresholds, or cumulative thresholds, for example, periods where temperatures remain above the 90th percentile for an extended period of at least five days (Hobday et al., 2016; Scannell et al., 2016; Hobday et al., 2018). In contrast, marine cold waves (MCWs) are defined as anomalously cold events characterized by sustained temperatures that remain below the 10th percentile for an extended period (Hobday et al., 2016; Hobday et al., 2018; Schlegel et al., 2021; Wang et al., 2022). It is important to note that these events are known by various other names (Schlegel et al., 2021); however, in this study, we will utilize the terms "marine heatwaves (MHWs)" and "marine cold waves (MCWs)." Both MHW and MCW occur in regions such as the North Atlantic, North Pacific, South China Sea, Mediterranean Sea, and other marine areas, leading to significant ecological disasters and economic losses on a global scale (Scannell et al., 2016, Smale et al., 2019; Wang et al., 2022; Smith et al., 2023; Li et al., 2024; Deser et al., 2024; Lubitz et al., 2024). In recent decades, the rate of warming in the South China Sea has significantly exceeded the global average, resulting in an increase in the frequency and intensity of extreme high temperature events (Hobday et al., 2018; Oliver et al., 2019; Li et al., 2022). Research indicates that the occurrence of MHWs in the South China Sea displays pronounced spatial and seasonal variability, with the anomalously strong Western Pacific Subtropical High (WPSH) identified as a key factor influencing the incidence of MHWs during both summer and winter (Li et al., 2022; Wang et al., 2022; Gao et al., 2023; Wang et al., 2023). Conversely, the frequency of MCWs in the South China Sea is declining and characterized by a spatially uneven distribution (Li et al., 2024).

MHWs and MCWs not only affect ecosystems but also exert a significant influence on the marine carbon cycle (Zang et al., 2018; Li et al., 2024). Within the global carbon cycle, the ocean functions as a major carbon sink, playing a crucial role in regulating Earth's climate (Le et al., 2010; Laruelle et al., 2018; Friedlingstein et al.,

2022; Dong et al., 2022). Since the onset of the industrial revolution, the ocean has absorbed approximately 25% of the anthropogenic carbon emissions (Raven and Falkowski, 1999; Takahashi et al., 2009; Friedlingstein et al., 2022; DeVries, 2022; Gruber et al., 2023; DeVries et al., 2023). Although marginal seas comprise only 8% of the global ocean area, they contribute 28% of primary productivity, absorbing approximately 0.2-0.4 Pg C of CO_2 annually, thereby significantly impacting global ocean carbon uptake (Borges et al., 2005; Chen and Borges, 2009; Dai et al., 2013; Laruelle et al., 2018). The South China Sea, as a significant marginal sea, is an integral component of the marine carbon cycle (Bopp et al., 2009; Le et al., 2010; Dai et al., 2022). Various factors influence the carbon cycle across different SCS regions of the South China Sea. For example, the South China Sea basin is predominantly influenced by vertical and horizontal transport through the Luzon Strait, while the northern coastal areas are impacted by the Pearl River, Kuroshio Current, Min-Zhe coastal current, coastal upwelling, and phytoplankton growth (Dai et al., 2009, 2013; Sun et al., 2014; Ye et al., 2017; Dai and Meng, 2020; Meng et al., 2024).

The exchange of CO_2 at the air-sea interface is a key process in the marine carbon cycle (DeVries, 2022). Under the influence of MHW, the solubility of CO_2 in seawater decreases, while the strengthening of monsoons limits the growth of phytoplankton, reducing the effectiveness of the marine biological pump (Chen et al., 2024). These changes affect the exchange of CO_2 between the ocean and the atmosphere, weakening the ability of the ocean to mitigate climate change by absorbing CO_2 and potentially shifting the ocean from a CO_2 sink to a CO_2 source, whereas MCWs have the opposite effect (Hobday et al., 2018; Zang et al., 2018; Aoki et al., 2021; Noh et al., 2022; Mignot et al., 2022; Edwing et al., 2024; Li et al., 2024). The South China Sea overall exhibits characteristics of a weak carbon source (Zhai et al., 2013; Li et al., 2020). While studies have explored factors influencing the CO_2 flux between the sea and air in the South China Sea, such as nutrient influx from northern rivers enhancing phytoplankton carbon fixation (Hung et al., 2020; Zhao et al., 2021), intensified upwelling of subsurface waters releasing CO_2 in the southeastern sea area off Taiwan during winter (Zhai et al., 2013), and typhoons enhancing CO_2 emissions from the

South China Sea to the atmosphere (Yu et al., 2020; Meng et al., 2024), no research has examined the impact of MHWs and MCWs on surface seawater CO_2 partial pressure (pCO_{2sea}) and air-sea CO_2 flux (FCO_2) in the South China Sea. Therefore, this study aims to quantify the changes in pCO_{2sea} and FCO_2 during MHWs and MCWs in the South China Sea and explore their potential mechanisms. Using existing pCO_{2sea} inversion data (Song et al., 2023) and reanalysis wind field data, we investigated the patterns of changes in pCO_{2sea} and FCO_2 from 2003 to 2019 during MHWs and MCWs and attempt to elucidate the underlying mechanisms.

The remainder of this article is structured as follows: Section 2 provides an overview of the data and analysis methods; Section 3 analyzes the changes in FCO_2 and pCO_2 during MHWs and MCWs in the South China Sea and their causes; and Section 4 summarizes the findings of this study.

2、Data and Methods

2.1 Data

This study utilized multiple datasets to investigate variables such as pCO_{2sea}, FCO_2, atmospheric carbon dioxide partial pressure (pCO_{2air}) , sea surface temperature (SST), sea surface salinity (SSS), chlorophyll-a (chl-a) concentration, and wind speed (U10). The details of the data are as follows:

Monthly mean pCO_{2sea} data, spanning from 2003 to 2019 with a spatial resolution of 1 km, were provided by Song et al., (2023). The pCO_{2air} data were sourced from the National Oceanic and Atmospheric Administration (NOAA) National Centers for Environmental Information, utilizing a combination of observational data and neural network methods, with a spatial resolution of 1°×1° (Landschützer et al., 2016). SST data were obtained from the global Optimum Interpolation Sea Surface Temperature (OISST) dataset, provided by NOAA, covering the period from December 1981 to the present, with a spatial resolution of 0.25°×0.25° (Reynolds et al., 2007). The SSS data were sourced from the Copernicus Marine Environment Monitoring Service (CMEMS) GLOBal-REANal. YSISPHY-001-030 product, with a

spatial resolution of 0.083° × 0.083° and monthly mean data from January 1993 to the present. Chl-a data were obtained from MODIS-Aqua, with a spatial resolution of 4km, covering the period from July 2002 to the present. U10 data comes from the ERA5 dataset provided by the European Center for Medium-Range Weather Forecasts (ECMWF), with a spatial resolution of 0.25° × 0.25° and a time span from January 1979 to the present.

2.2 MHW and MCW detection method

According to Hobday et al., (2016), an MHW is defined as an anomalously warm event where the sea surface temperature exceeds the 90th percentile and persists for five days or longer, while an MCW is defined as an anomalously cold event where the sea surface temperature falls below the 10th percentile and persists for five days or longer. To account for potential ecological effects of temperature variations in different seasons, daily sea surface temperature anomalies were calculated by removing the seasonal cycle (subtracting the long-term climatological mean sea surface temperature for each day). This approach allows the thresholds to vary with seasons, enabling the detection of summer MHW and winter warm spells, which is crucial for studying the potential impacts of different seasons on ecosystems. Furthermore, for each day of each year, climatological thresholds and means were calculated using daily temperature values from all years and values within an 11-day window centered on that day. Subsequently, a 31-day moving window was applied for smoothing, which helped eliminate short-term noise and fluctuations and made the data smoother and more reliable. Owing to the limitations of the existing pCO_{2sea} inversion data, which comprise only monthly data from 2003 to 2019, we define months in which the number of MHW days or MCW days exceeds 15 as MHW months and MCW months, respectively. Our study focuses on these months, which are characterized by significant MHW and MCW events.

Furthermore, the detection of MHW and MCW generally requires at least 30 years of SST data. To ensure the reliability and scientific validity of our analytical

results, we detected MHW and MCW using OISST data spanning January 1990 to December 2019.

2.3 Diagnostic analysis method

The calculation of FCO_2 is as follows:

$$FCO_2 = K \times K_H \times (pCO_{2sea} - pCO_{2air})$$ （1）

In the equation 1, K represents the gas transfer velocity, and K_H is the solubility of CO_2 in seawater (Weiss, 1974, Wanninkhof, 1992). pCO_{2sea} and pCO_{2air} are the partial pressures of CO_2 in the ocean and the atmosphere, respectively. A positive value of FCO_2 value indicates that CO_2 is transferred from the ocean to the atmosphere, suggesting that the ocean is a source of CO_2 to the atmosphere. Conversely, a negative value indicates that CO_2 is transferred from the atmosphere to the ocean, suggesting that the ocean acts as a sink for CO_2.

To understand which factor (ΔpCO_2 (pCO_{2sea}-pCO_{2air}) or wind speed (Γ)) dominates the FCO_2 anomaly during the MHWs, MCWs and normal conditions periods, we decomposed the FCO_2 anomaly in the northern South China Sea. Each flux component is considered the sum of its long-term mean and anomaly values (Edwing et al., 2024), therefore, the decomposition is as follows:

$$FCO_2{}' = \overline{(\Gamma)}\left(\Delta pCO_2{}'\right) + \overline{(\Delta pCO_2)}\left(\Gamma'\right) + (O_2)$$ （2）

In Equation 2, the terms on the right-hand side represent the contributions of the ΔpCO_2 anomaly, wind speed anomaly, and a negligible higher-order residual term O_2. The factor with the largest anomaly contribution is the primary driver of the FCO_2 anomaly. Additionally, to separate the influence of SST (MHW) on the pCO_{2sea} anomaly (pCO_{2sea}'), we calculated the temperature-induced pCO_{2sea}' （$pCO_{2T}{}'$） and non-temperature-induced pCO_{2sea}' （$pCO_{2NT}{}'$） .

$$pCO_{2T}{}' = \overline{pCO_2} * \exp\left(0.0423(SST - \overline{SST})\right) - \overline{pCO_2}$$ （3）

$$pCO_{2NT}' = pCO_2 * \exp\left(0.0423(\overline{SST} - SST)\right) - \overline{pCO_2} \qquad (4)$$

In Equation 3 and 4, $\overline{pCO_2}$ and $\overline{SST}$ represent the climatological baseline values of pCO_{2sea} and SST, respectively. The variability coefficient of pCO_{2sea} was set to 0.0423 °C^{-1} (Takahashi et al., 1993, 2002). The temperature component represents the pCO_{2sea}' driven by SST changes, whereas the non-temperature component includes pCO_{2sea}' caused by dissolved inorganic carbon (DIC), total alkalinity (TA), and SSS. The factors influencing the non-temperature component include biological activity (Cao et al., 2020; Signorini et al., 2013), physical transport and mixing (Cao et al., 2020; Jiang et al., 2008), and air-sea gas exchange (Cai et al., 2020).

3、 Results

3.1 Detection of MHWs and MCWs in the South China Sea from 2003 to 2019
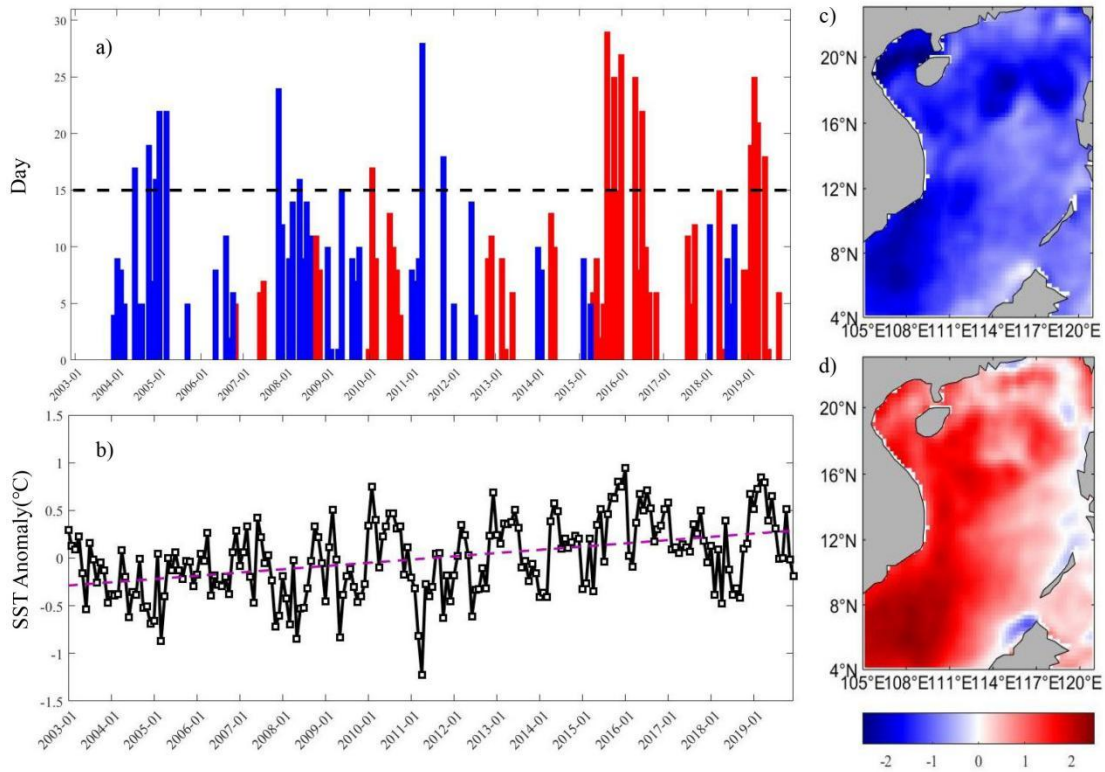

Fig. 1. (a) Monthly durations of MHWs and MCWs, and (b) monthly SST anomalies from 2003 to 2019. The black dashed line marks the 15-day threshold, and the purple dashed line shows the trend in SST anomalies. Spatial distribution of SST anomalies in the South China Sea during (c)

the MCW in April 2011 and (d) the MHW in January 2016.

Fig. 1a indicates an increasing frequency of MCWs, whereas the frequency of MHWs decreases. This trend was further emphasized by SST anomalies. As depicted in Fig. 1b, the SST anomaly in April 2011 was the highest for the MCW months from 2003 to 2019, and the SST anomaly in January 2016 was the highest for the MHW months from 2003 to 2019. Additionally, Fig. 1c and d illustrates that SST anomalies were more pronounced along the southern coast of Vietnam during these extreme anomaly periods. During the extreme MCW period, SST anomalies were also more significant in the Bashi Channel and northern part of the Gulf of Tonkin. Furthermore, to investigate the response of FCO_2 to MHWs and MCWs in the northern South China Sea, we focused on the MHW in January 2016 and the MCW in April 2011. By studying the variations in FCO_2 during these two extreme events, we can gain an initial understanding of the impacts of MHWs and MCWs on FCO_2.
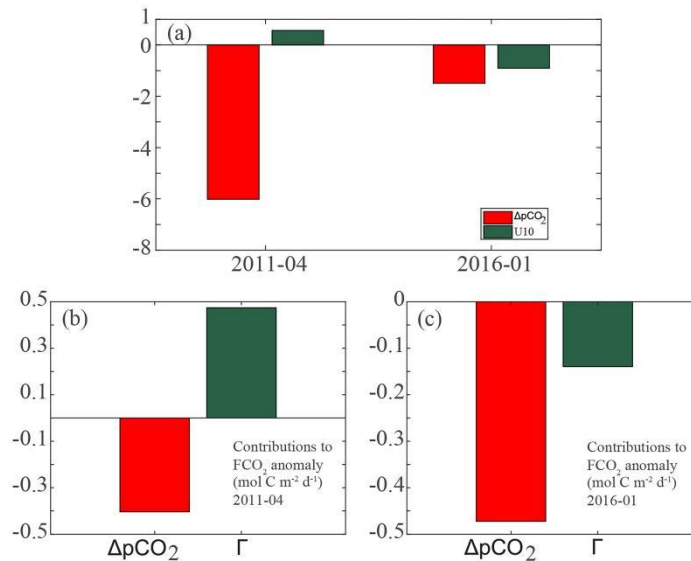

Fig. 2. (a) Anomalies of $\Delta pCO2$ and U10. Contributions of $\Delta pCO2$ and U10 to the anomalies of FCO2 during (b) the MCW in April 2011 and (c) the MHW in January 2016. Red bars represent MHWs, while blue bars represent MCWs.

During the MCW in April 2011, as shown in Fig. 2a, ΔpCO_2 decreased by 6.02 µatm, while wind speed increased by 0.56 m/s. Conversely, in January 2016, ΔpCO_2 decreased by 1.50 µatm, accompanied by a decrease in the wind speed of 0.91 m/s. Fig. 2b and c indicate that during the April 2011 cold wave event, FCO$_2$ driven by Δ

pCO_2 decreased, whereas FCO_2 driven by U10 increased. In contrast, during the heat wave event in January 2016, both ΔpCO_2-driven FCO_2 and wind-driven FCO_2 decreased.

3.2 Variations in the impact of MHWs and MCWs on FCO_2 in the South China Sea from 2003 to 2019

Over the 17-year period from 2003 to 2019, the average FCO_2 in the South China Sea was positive—approximately 1.2 mol C m^{-2} d^{-1} during MHWs, 1.3 mol C m^{-2} d^{-1} under normal conditions, and 0.9 mol C m^{-2} d^{-1} during MCWs—indicating that the South China Sea generally acted as a weak source of atmospheric CO_2. Furthermore, as shown in Fig. 3a-c, the changes in FCO_2 during MHWs and MCWs revealed a mean FCO_2 anomaly of +0.1530 mmol/m^2/d, which is higher than the mean FCO_2 anomaly of -0.0082 mmol/m^2/d under normal conditions. This suggests that MHWs in the South China Sea lead to an increase in FCO_2, thereby enhancing the capacity of the sea to release CO_2. Conversely, during the MCWs, the mean FCO_2 anomaly was -0.1561 mmol/m^2/d, which is lower than the mean FCO_2 anomaly under normal conditions. This indicates that the MCWs in the South China Sea led to a decrease in FCO_2, thereby reducing the capacity of the sea to release CO_2.
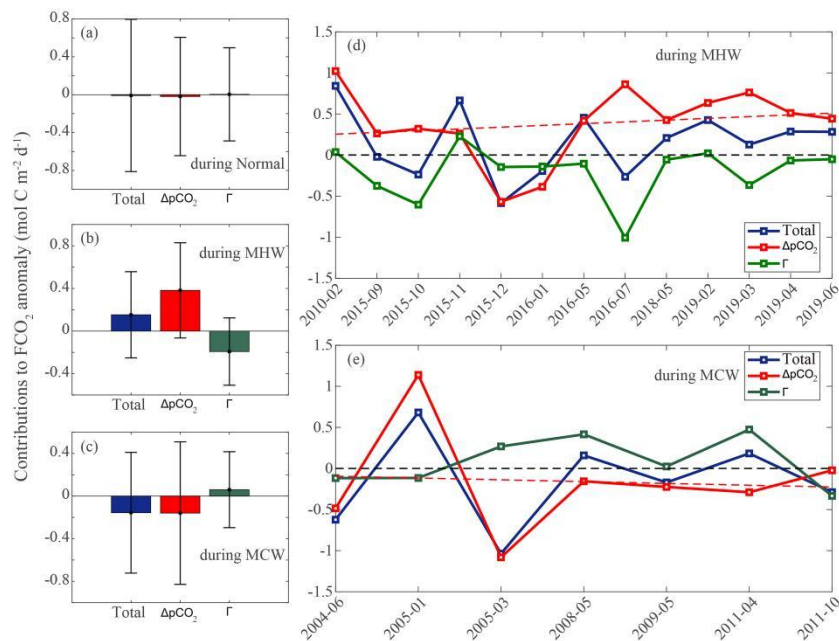

Fig. 3. The Impacts of MHWs and MCWs on FCO_2 in the South China Sea from 2003 to 2019.

Contributions of ΔpCO_2 and U10 (Γ) to FCO_2 anomaly during (a) Normal conditions, (b, d) MHWs and (c, e) MCWs from 2003 to 2019. The red dashed line represents the trend of FCO_2 anomalies driven by ΔpCO_2, while the black dashed line represents the zero value line.

To further distinguish the contributions of ΔpCO_2 and U10 to the variations in FCO_2 during MHWs and MCWs in the South China Sea, we quantified their mean contributions to FCO_2 from 2003 to 2019. As shown in Fig. 3a-c, during normal conditions, the variation in FCO_2 driven by ΔpCO_2 was -0.02 ± 0.62 mmol/m^2/d, and the variation driven by U10 was $+0.004 \pm 0.50$ mmol/m^2/d. However, during MHWs, the variation in FCO_2 driven by ΔpCO_2 was $+0.38 \pm 0.45$ mmol/m^2/d, while that driven by U10 was -0.20 ± 0.32 mmol/m^2/d. In contrast, during MCWs, the variation in FCO_2 driven by ΔpCO_2 was -0.16 ± 0.67 mmol/m^2/d, and that driven by U10 was $+0.06 \pm 0.36$ mmol/m^2/d. This indicates that during MHWs, changes in ΔpCO_2 enhance the emission of CO_2 from the South China Sea, while changes in wind speed weaken this process, with the opposite occurring during MCWs. Furthermore, prior to May 2018, the South China Sea alternated between being a carbon source and a carbon sink during MHWs, but predominantly acted as a carbon source afterwards. This transition is likely related to increased ΔpCO_2, which is possibly associated with ocean warming. During MCWs, the South China Sea acted as a carbon sink. Overall, ΔpCO_2 was the dominant factor influencing FCO_2 variation relative to wind speed. MCWs reduce CO_2 release in the South China Sea, whereas MHWs increase CO_2 release.

As illustrated in Fig. 3d and e, during MHWs, changes in FCO_2 driven by ΔpCO_2 exhibited an increasing trend, indicating that variations in ΔpCO_2 enhanced the CO_2 emissions from the South China Sea. Conversely, during MCWs, there was a decreasing trend in FCO_2 changes driven by ΔpCO_2, suggesting that ΔpCO_2 variations reduced CO_2 emissions in the South China Sea. Notably, between May 2008 and October 2011, during the MCWs, the rate of negative change in FCO_2 driven by ΔpCO_2 diminished, which may be associated with ocean warming. Additionally, during MHWs, the correlation coefficient between the ΔpCO_2-driven variation of FCO_2 and the total variation of FCO_2 is 0.5950, while the correlation

coefficient between the U10-driven variation of FCO_2 and the total variation of FCO_2 is 0.5185, indicating a similar level of impact. In contrast, during MCWs, the correlation coefficient between the ΔpCO_2-driven variation of FCO_2 and the total variation of FCO_2 was significantly higher at 0.8761, compared to the correlation coefficient between the U10-driven variation of FCO_2 and the total variation of FCO_2, which is 0.1206. This suggests that the impact of ΔpCO_2 on FCO_2 was more pronounced during MCWs than during MHWs.

3.3 Variations in the impact of MHWs and MCWs on pCO_{2sea} in the South China Sea from 2003 to 2019

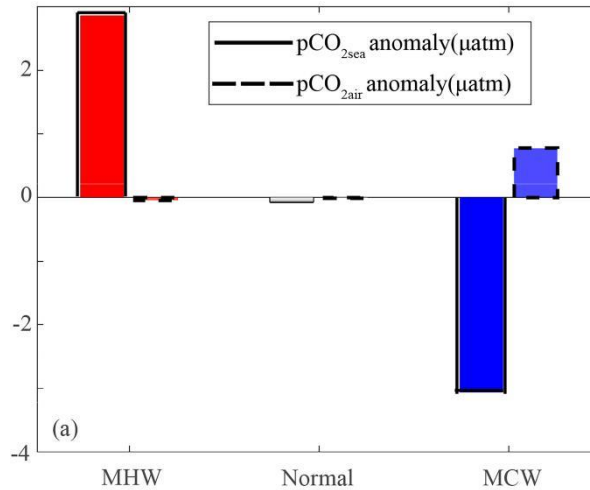Fig. 4. Anomalies of pCO_{2sea} and pCO_{2air} during normal conditions, MHWs, and MCWs in the

South China Sea.

The change in ΔpCO_2 was determined using the values of pCO_{2air} and pCO_{2sea}. As illustrated in Fig. 4, the pCO_{2air} anomaly values during MHWs (-0.05 µatm) and MCWs (0.77 µatm) are relatively close to the anomaly value during normal conditions (-0.02 µatm). In contrast, the pCO_{2sea} anomaly values during MHWs (+2.85 µatm) and MCWs (-3.06 µatm) exhibit more pronounced deviations from the anomaly value during normal conditions (-0.05 µatm). Therefore, changes in ΔpCO_2 were primarily influenced by variations in pCO_{2sea}.
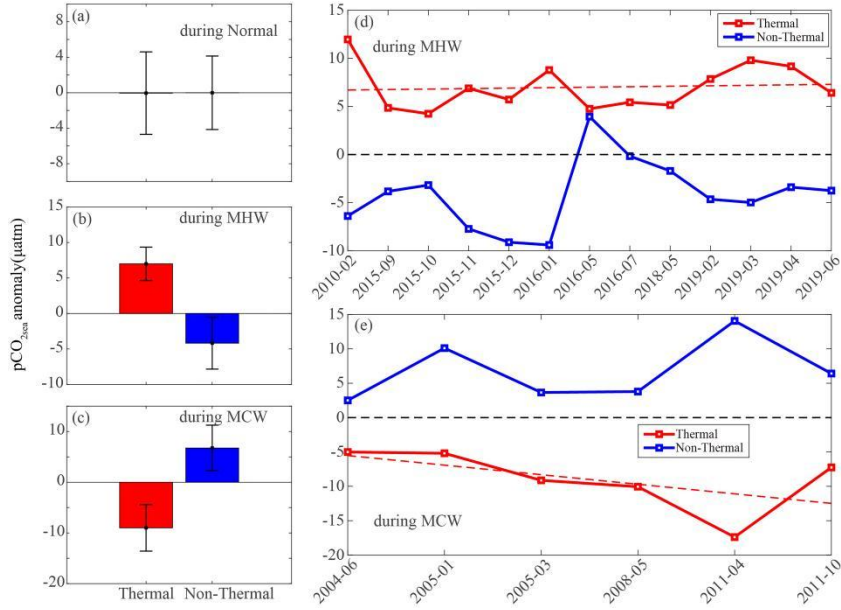
Fig. 5. The impacts of MHWs and MCWs on pCO_{2sea} in the South China Sea from 2003 to 2019. Anomalies of pCO_{2sea} caused by temperature and non-temperature factors during (a) normal conditions, (b, d) MHWs and (c, e) MCWs. The red dashed line indicates the trend of pCO_2 changes attributed to temperature factors, while the black dashed line represents the zero value line.

Furthermore, we investigated the main factors affecting pCO_{2sea} during MHWs and MCWs in the South China Sea. As shown in Fig. 5, during normal conditions, the impacts of temperature and non-temperature factors on pCO_{2sea} anomalies were relatively small, at -0.04 ± 4.64 μatm and -0.01 ± 4.14 μatm, respectively. During MHWs, temperature factors contributed significantly to increases in pCO_{2sea}, with an average value of $+7.00 \pm 2.35$ μatm, while non-temperature factors reduced pCO_{2sea}, averaging -4.18 ± 3.65 μatm. Conversely, during MCWs, temperature factors caused a decrease in pCO_{2sea} (-9.00 ± 4.58 μatm), whereas non-temperature factors led to an increase ($+6.75 \pm 4.50$ μatm). Overall, temperature factors were the primary drivers of changes in pCO_{2sea} during both MHWs and MCWs, with their impact gradually increasing over time.
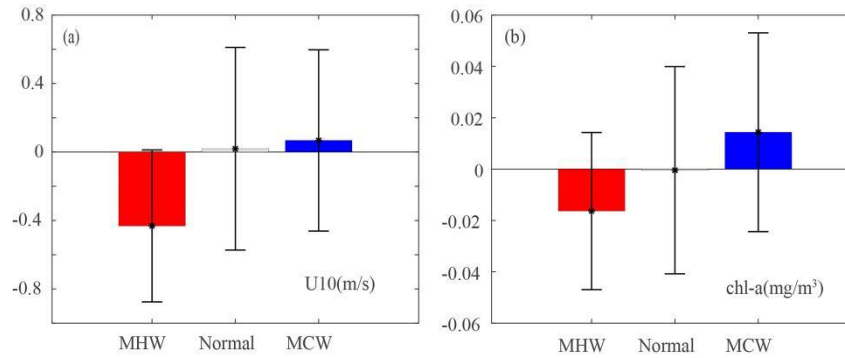
4、Discussion

Fig. 6. Anomalies of (g) U10 and (h) chl-a during normal conditions, MHWs, and MCWs from 2003 to 2019.

As shown in Fig. 6a, wind speed during MCWs increased (+0.05m/s) compared to normal conditions, but decreased significantly during MHWs (-0.45 m/s). Reduced wind speed can weaken the surface wind stress, thereby suppressing vertical mixing and physical transport in the upper ocean (DeVries, 2022; Meng et al., 2024). This promotes stronger stratification, limits nutrient supply, and reduces the upwelling of deep DIC, typically leading to a decrease in pCO_{2sea} in surface waters. Moreover, reduced wind speed can also decrease the heat exchange between the ocean and atmosphere, lowering latent and sensible heat fluxes transferred from the ocean surface to the atmosphere, which may result in an increase in sea surface temperature.

MHWs and MCWs may also affect the growth of surface phytoplankton, which consume CO_2 at the sea surface (Chen et al., 2024). To explore this further, we investigated the changes in surface chl-a concentration during these two periods. As shown in Fig. 6b, compared to normal conditions (0 mg/m^3), the concentration of chl-a during MHWs (-0.02 mg/m^3) decreased, potentially reducing CO_2 consumption at the sea surface and indirectly an increasing in pCO_{2sea}. Meanwhile, lower wind speeds during MHWs could have led to reduced physical transport and mixing, which may have resulted in a decrease in the pCO_{2sea}. Conversely, during MCWs, chl-a concentrations (+0.01 mg/m^3) increased, likely enhancing CO_2 consumption at the sea surface and indirectly decreasing pCO_{2sea}. Additionally, the increased wind speeds during MCWs may have enhanced physical transport and mixing, contributing to the observed increase in the pCO_{2sea}. Thus, the primary factor influencing the non-temperature-driven pCO_{2sea} during both MHWs and MCWs is more likely related

to physical processes, such as seawater mixing and advection.

5、Conclusion

As a marginal sea, the findings from the South China Sea may provide important insights into the impacts of MHWs and MCWs on FCO_2 in the global ocean. Using inverted data, we conducted the first investigation into the effects of MHWs and MCWs on FCO_2 in the South China Sea from 2003 to 2019. Our findings indicate that the South China Sea functions as a weak carbon source during this period and is frequently subjected to MHWs while occasionally experiences MCWs, both of which affect the air-sea CO_2 flux:

1、The capacity of the South China Sea to release CO_2 tends to increase during the MHWs and decrease during the MCWs, with FCO_2 rising during MHWs and falling during MCWs.

2、These changes in FCO_2 during MHWs and MCWs were primarily driven by ΔpCO_2 rather than by wind speed, with variations in pCO_{2sea} playing a crucial role.

3、During MHWs and MCWs, temperature played a dominant role in influencing pCO_{2sea}, driving an increase during MHWs and a decrease during MCWs, with its impact gradually increasing over time.

In future research, we will investigate the combined effects of various extreme weather events on the CO_2 absorption in the South China Sea. Additionally, we will employed numerical model simulations to explore the dynamic mechanisms driving the impact of MHWs and MCWs on CO_2 absorption across different regions of the South China Sea, analyzing potential regional differences and their underlying causes.

Conflict of Interest

The authors declare that they have no conflict of interests.

References

1. Amaya D J, Jacox M G, Alexander M A, et al. Bottom marine heatwaves along the continental shelves of North America. Nat. Commun. 2023; 14(1):1038.

2. Aoki L R, McGlathery K J, Wiberg P L, et al. Seagrass recovery following marine heat wave influences sediment carbon stocks. Front. Mar. Sci. 2021; 7:576784.

3. Bopp L, Le Quéré C. Ocean carbon cycle. Geophys. Monogr. Ser. 2009; 187:181-195.

4. Borges A V, Delille B, Frankignoulle M. Budgeting sinks and sources of CO_2 in the coastal ocean: Diversity of ecosystems counts. Geophys. Res. Lett. 2005; 32(14).

5. Cao Z, Yang W, Zhao Y, et al. Diagnosis of CO_2 dynamics and fluxes in global coastal oceans. Natl. Sci. Rev. 2020; 7(4): 786-797.

6. Chen C T A, Borges A V. Reconciling opposing views on carbon cycling in the coastal ocean: Continental shelves as sinks and near-shore ecosystems as sources of atmospheric CO_2. Deep Sea Res. Part II. 2009; 56(8-10):578-590.

7. Chen Y, Shen C, Zhao H, et al. The impact of marine heatwaves on surface phytoplankton chlorophyll-a in the South China Sea. Sci. Total Environ. 2024; 949:175099.

8. Dai M, Su J, Zhao Y, et al. Carbon fluxes in the coastal ocean: synthesis, boundary processes, and future trends. Annu. Rev. Earth Planet. Sci. 2022; 50(1):593-626.

9. Deser C, Phillips A S, Alexander M A, et al. Future Changes in the Intensity and Duration of Marine Heat and Cold Waves: Insights from Coupled Model Initial-Condition Large Ensembles. J. Climate 2024; 37(6):1877-1902.

10. DeVries T, Yamamoto K, Wanninkhof R, et al. Magnitude, trends, and variability of the global ocean carbon sink from 1985 to 2018. Glob. Biogeochem. Cycles 2023; 37(10):e2023GB007780.

11. DeVries T. The ocean carbon cycle. Annu. Rev. Environ. Resour. 2022; 47(1):317-341.

12. Dong Y, Bakker D C, Bell T G, et al. Update on the temperature corrections of global air-sea CO_2 flux estimates. Global Biogeochem. Cycles. 2022; 36(9):e2022GB007360.

13. Edwing K, Wu Z, Lu W, et al. Impact of marine heatwaves on Air-Sea CO2 Flux Along the US East Coast. Geophys. Res. Lett. 2024; 51(1):e2023GL105363.

14. Frölicher T L, Fischer E M, Gruber N. Marine heatwaves under global warming. Nat. 2018; 560(7718):360-364.

15. Gao Z, Jia W, Zhang W. Study on Seasonal Characteristics and Causes of marine heatwaves in the South China Sea over Nearly 30 Years. Atmos. 2023; 14(12):1822.

16. Gruber N, Bakker D C, DeVries T, et al. Trends and variability in the ocean carbon sink. Nat. Rev. Earth Environ. 2023; 4(2):119-134.

17. Hobday A J, Alexander L V, Perkins S E, et al. A hierarchical approach to defining marine heatwaves. Prog. Oceanogr. 2016; 141:227-238.

18. Hobday A J, Oliver E C, Gupta A S, et al. Categorizing and naming marine heatwaves. Oceanogr. 2018; 31(2):162-173.

19. Hung J J, Wang Y J, Tseng C M,et al. Controlling mechanisms and cross linkages of ecosystem metabolism and atmospheric CO_2 flux in the northern South China Sea. Deep Sea Res. Part I. 2020; 157:103205.

20. Jiang L Q, Cai W J, Wanninkhof R. Air-sea CO_2 fluxes on the US South Atlantic Bight: Spatial and seasonal variability. J. Geophys. Res. Oceans. 2008; 113(C7):C07019.

21. Landschützer P, Gruber N, Bakker D C. Decadal variations and trends of the global ocean carbon sink. Glob. Biogeochem. Cycles. 2016; 30(10):1396-1417.

22. Laruelle G G, Cai W J, Hu X, et al. Continental shelves as a variable but increasing global sink for atmospheric carbon dioxide. Natur. Commun. 2018; 9(1):454.

23. Le Quéré C, Takahashi T, Buitenhuis E T, et al. Impact of climate change and variability on the global oceanic sink of CO_2. Glob. Biogeochem. Cycles. 2010; 24(4):GB4007.

24. Li Y, Ren G, Wang Q, et al. Marine heatwaves in the South China Sea: tempo-spatial pattern and its association with large-scale circulation. Remote Sens. 2022; 14(22):5829.

25. Li Q, Guo X, Zhai W, et al. Partial pressure of CO_2 and air-sea CO_2 fluxes in the South China Sea: Synthesis of an 18-year dataset. Prog. Oceanogr. 2020; 182:102272.

26. Li H, Lu J, Tong H, et al. Impact of high temperature heat waves on ocean carbon sinks: Based on literature analysis perspective. J. Sea Res. 2024; 198:102487.

27. Li C, Sun W, Ji J, et al. Historical Marine Cold Spells in the South China Sea: Characteristics and Trends. Remote Sens. 2024; 16(7):1171.

28. Lubitz N, Daly R, Smoothey A F, et al. Climate change-driven cooling can kill marine megafauna at their distributional limits. Nature Clim. Chang. 2024; 14:526–535.

29. Luo M, Lau N C, Liu Z, et al. An observational investigation of spatiotemporally contiguous heatwaves in China from a 3D perspective. Geophys. Res. Lett. 2022; 49(6):e2022GL097714.

30. Meng Z, Guan Y, Feng Y. Simulating the impact of typhoons on air-sea CO_2 fluxes on the northern coastal area of the South China Sea. Environ. Res. Lett. 2024; 19(4):044008.

31. Mignot A, Von Schuckmann K, Landschützer P, et al. Decrease in air-sea CO_2 fluxes caused by persistent marine heatwaves. Nat. Commun. 2022; 13(1):4300.

32. Noh K M, Lim H G, Kug J S. Global chlorophyll responses to marine heatwaves in satellite ocean color. Environ. Res. Lett. 2022; 17(6):064034.

33. Oliver E C, Benthuysen J A, Darmaraki S, et al. Marine heatwaves. Annu. Rev. Mar. Sci. 2021; 13(1):313-342.

34. Oliver E C, Burrows M T, Donat M G, et al. Projected marine heatwaves in the 21st century and the potential for ecological impact. Front. Mar. Sci. 2019; 6:734.

35. Oliver E C, Donat M G, Burrows M T, et al. Longer and more frequent marine heatwaves over the past century. Nat. Commun. 2018; 9(1):1-12.

36. Raven J A, Falkowski P G. Oceanic sinks for atmospheric CO_2. Plant Cell Environ. 1999; 22(6):741-755.

37. Reynolds R W, Rayner N A, Smith T M, et al. An improved in situ and satellite SST analysis for climate. J. Climate., 2002. 15(13): 1609-1625.

38. Reynolds R W, Smith T M, Liu C, et al. Daily high-resolution-blended analyses for sea surface temperature. J. Climate. 2007; 20(22): 5473-5496.

39. Scannell H A, Pershing A J, Alexander M A, et al. Frequency of marine heatwaves in the North Atlantic and North Pacific since 1950. Geophys. Res. Lett. 2016; 43(5):2069-2076.

40. Schlegel R W, Darmaraki S, Benthuysen J A, et al. Marine cold-spells. Prog. Oceanogr. 2021; 198:102684.

41. Signorini S R, Mannino A, Najjar Jr, et al. Surface ocean pCO_2 seasonality and sea-air CO_2 flux estimates for the North American east coast. J. Geophys. Res. Oceans. 2013; 118(10):5439-5460.

42. Smale D A, Wernberg T, Oliver E C, et al. Marine heatwaves threaten global biodiversity and the provision of ecosystem services. Nat. Clim. Change. 2019; 9(4):306-312.

43. Smith K E, Burrows M T, Hobday A J, et al. Biological impacts of marine heatwaves. Annu. Rev. Mar. Sci. 2023; 15(1):119-145.

44. Song Z, Yu S, Bai Y, et al. Construction of a high spatiotemporal resolution dataset of satellite-derived pCO_2 and air-sea CO_2 flux in the South China Sea (2003-2019). IEEE Trans. Geosci. Electron. 2023; 61:1-15.

45. Sun Q, Tang D, Legendre L, et al. Enhanced sea-air CO_2 exchange influenced by a tropical depression in the South China Sea. J. Geophys. Res. Oceans. 2014; 119(10):6792-6804.

46. Takahashi T, Olafsson J, Goddard J G, et al. Seasonal variation of CO2 and nutrients in the high-latitude surface oceans: A comparative study. Global Biogeochem. Cycles. 1993; 7(4):843-878.

47. Takahashi T, Sutherland S C, Sweeney C, et al. Global sea–air CO_2 flux based on climatological surface ocean pCO_2, and seasonal biological and temperature effects. Deep Sea Res. Part II. 2002; 49(9-10):1601-1622.

48. Takahashi T, Sutherland S C, Wanninkhof R, et al. Climatological mean and decadal change in surface ocean pCO_2, and net sea–air CO_2 flux over the global oceans. Deep Sea Res. Part II. 2009; 56(8-10):554-577.

49. Wang G, Wu L, Mei W, et al. Ocean currents show global intensification of weak tropical cyclones. Nature. 2022; 611(7936):496-500.

50. Wang Q, Zhang B, Zeng L, et al. Properties and drivers of marine heat waves in the northern South China Sea. J. Phys. Oceanogr. 2022; 52(5):917-927.

51. Wang Y, Kajtar J B, Alexander L V, et al. Understanding the changing nature of marine cold-spells. Geophys. Res. Lett. 2022; 49: e2021GL097002.

52. Wang Y, Zhang C, Tian S, et al. Seasonal cycle of marine heatwaves in the northern South China Sea. Clim. Dyn. 2023; 61(7):3367-3377.

53. Wanninkhof R. Relationship between wind speed and gas exchange over the ocean. J. Geophys. Res. Oceans. 1992; 97(C5):7373-7382.

54. Weiss R. Carbon dioxide in water and seawater: the solubility of a non-ideal gas. Mar. Chem. 1974; 2(3):203-215.

55. Ye F, Guo W, Shi Z, et al. Seasonal dynamics of particulate organic matter and its response to flooding in the Pearl River E stuary, China, revealed by stable isotope ($\delta 13$ C and $\delta 15$ N) analyses. J. Geophys. Res. Oceans. 2017; 122(8):6835-6856.

56. Yu P, Wang Z A, Churchill J, et al. Effects of typhoons on surface seawater pCO_2 and air-sea CO_2 fluxes in the northern South China Sea. J. Geophys. Res. Oceans. 2020; 125(8):e2020JC016258.

57. Zhao H, Dai M, Gan J, et al. River-dominated pCO_2 dynamics in the northern South China Sea during summer: A modeling study. Prog. Oceanogr. 2021; 190:102457.

58. Zhai W D, Dai M H, Chen B S, et al. Seasonal variations of sea–air CO_2 fluxes in the largest tropical marginal sea (South China Sea) based on multiple-year underway measurements. Biogeosciences. 2013; 10(11):7775-7791.

59. Zang H, Li Y, Xue L, et al. The contribution of low temperature and biological activities to the CO_2 sink in Jiaozhou Bay during winter. J. Mar. Syst. 2018; 186:37-46.